Life Sciences 228 (2019) 305–315

Contents lists available at ScienceDirect

Life Sciences

journal homepage: www.elsevier.com/locate/lifescie

Silymarin protects against radiocontrast-induced nephropathy in mice

Verônica de Souza Santos[a], Beatriz Peters[a], Larissa Zambom Côco[a], Gisele Maziero Alves[a], Arícia Leone Evangelista Monteiro de Assis[b], Breno Valentim Nogueira[b], Silvana Santos Meyrelles[c], Marcella Leite Porto[d], Elisardo Corral Vasquez[a,c], Bianca Prandi Campagnaro[a], Thiago Melo Costa Pereira[a,d,*]

[a] Pharmaceutical Sciences Graduate Program, Vila Velha University (UVV), Vila Velha, ES, Brazil
[b] Department of Morphology, Health Sciences Center, Federal University of Espirito Santo, Vitoria, Brazil
[c] Laboratory of Translational Physiology, Health Sciences Center, Federal University of Espirito Santo, Vitoria, Brazil
[d] Federal Institute of Education, Science and Technology (IFES), Vila Velha, ES, Brazil

ARTICLE INFO

Keywords:
Contrast-induced nephropathy (CIN)
Silymarin
Contrast renal toxicity
Oxidative stress
Apoptosis
Cystatin C

ABSTRACT

Silymarin, an extract from *Silybum marianum* (milk thistle) containing a standardized mixture of flavonolignans that ameliorates some types of liver disease and, more recently, kidney damage, could be used for the ROS-scavenging effect of these antioxidants. Furthermore, contrast-induced nephropathy (CIN) is an iatrogenic impairment of renal function in patients subjected to angiographic procedures for which there is not yet a successful preventative treatment. Recent evidence has shown that this event is related to tubular/vascular injury activated mainly by oxidative stress. However, whether this bioavailable and pharmacologically safe extract protects against CIN is not clear. We proposed to evaluate the possible protective role of the antioxidant silymarin in an experimental model of CIN. Adult male Swiss mice were separated into 6 groups and pretreated orally with silymarin (50, 200 and 300 mg/kg), *N*-acetylcysteine (200 mg/kg) or vehicle for 5 days before the CIN and control groups. Renal function was analyzed by plasma creatinine, urea and cystatin C levels. Additionally, blood reactive oxygen species (ROS) were evaluated using ROS bioavailability, protein oxidation and DNA damage. Renal oxidative damage was evaluated using apoptosis/cell viability assays and histological analysis. We showed that silymarin preserved renal function and decreased systemic and renal oxidative damage (antigenotoxic and antiapoptotic properties, respectively) in a dose-dependent manner and was superior to conventional treatment with *N*-acetylcysteine. Histologically, silymarin treatment also had beneficial effects on renal glomerular and tubular injuries. Therefore, silymarin prophylaxis may be an interesting strategy for the prevention of CIN.

1. Introduction

Contrast-induced nephropathy (CIN) is a result from iatrogenic deterioration of renal function mainly in vulnerable clinical subpopulations (e.g., elderly patients with dehydration, renal/cardiac dysfunction and/or diabetics) subjected to frequent angiographic procedures 2–5 days after administration of the intravascular contrast agent [1–3]. Although it is the third leading cause of all hospital-acquired renal insufficiency with high morbimortality, strategies to prevent CIN (e.g., hydration, reduction of contrast dose, sodium bicarbonate, and *N*-acetylcysteine) are still inadequate and subject patients to renal dysfunction and medical expenses [4–7]. In this context, the investigation of effective preventative interventions against CIN is fundamental to avoid kidney damage, costs and burden associated with this

Abbreviations: ANOVA, one-way analysis of variance; AOPP, advanced oxidation protein products; CCD, charge-coupled device; CIN, contrast-induced nephropathy; CM, contrast media; COX, cyclooxygenase; DHE, dihydroethidium; DCF, 2′,7′-dichlorofluorescein diacetate; HE, hematoxylin and eosin; HPF, 2-[6-(4′-hydroxy) phenoxy-3H-xanthen-3-on-9-yl]benzoic acid; hROS, highly reactive oxygen species; H_2O_2, hydrogen peroxide; L-NAME, L-NG-nitro arginine methyl ester; NAC, *N*-acetylcysteine; NO, nitric oxide; NOS, NO synthase; OM, optical microscopy; PBS, phosphate-buffered saline; PI, propidium iodide; ROS, reactive oxygen species; SEM, standard error of the mean; SEM, scanning electron microscopy; S50, silymarin 50 mg/kg; S200, silymarin 200 mg/kg; S300, silymarin 300 mg/kg; TILI, tubulointerstitial injury; V-FITC, fluorescein isothiocyanate-conjugated annexin V; $\cdot O_2^-$, superoxide; $\cdot OH^-$, hydroxyl radical; $\cdot ONOO^-$, peroxynitrite

* Corresponding author at: Laboratory of Translational Physiology and Pharmacology, Pharmaceutical Sciences Graduate Program, Vila Velha University (UVV), Av. Comissário José Dantas de Melo, n°21, 29102-920 Boa Vista, Vila Velha, ES, Brazil.
E-mail address: pereiratmc@gmail.com (T.M.C. Pereira).

https://doi.org/10.1016/j.lfs.2019.04.061

Available online 29 April 2019

complication [1,3,8].

The exact pathophysiology of CIN is still poorly understood [3,9]. Until now, it has been shown that iodinated contrast media (CM) develops a combination of renal vascular and tubular injury that is highly influenced by renal ischemia and ROS overproduction, culminating in oxidative stress, aggravation of renal vasoconstriction and apoptosis of kidney cells [1,3,10]. Moreover, CM can contribute to toxicity on renal tubular epithelial cells, as recently published by our group [1,4] and others [2,11–13]. The combination of these factors decreases the renal blood flow and glomerular filtration rate, culminating with progressive increases in renal biomarkers that characterize loss of renal function [3,10,13]. One of the top 10 most popular natural compounds used in Western society is silymarin, as noted by the exponential growth in publications indexed on the PubMed platform in the last decade [14]. This mixture contains 65% to 80% flavonolignans (silybin A, silybin B, isosilybin A, isosilybin B, silychristin and silydianin), with small amounts of flavonoids and polyphenolic compounds extracted from the seeds and fruits of *Silybum marianum* (milk thistle) [15,16]. Traditionally, silymarin has been used for the treatment of liver diseases by exploiting its potent strong antioxidative and antiapoptotic properties [14,16,17]. Considering the importance of these mechanisms in the progression of CIN [1,4,10], silymarin may be an interesting pharmacological strategy for the prevention of this complication. The confirmation of this hypothesis may promote a novel approach for preventing CIN.

2. Materials and methods

2.1. Animals

Experiments were conducted in male Swiss mice *Mus musculus* (30–45 g), maintained in the animal care facility at the Experimental Monitoring Laboratory of Vila Velha University (UVV), Espirito Santo, Brazil. The animals were fed a normal chow diet and water ad libitum and housed under standard conditions with a controlled temperature (~22 °C) and humidity (~60%) and were exposed to a 12/12-h light-dark cycle. All biological assays were performed in accordance with the guidelines for the care and handling of laboratory animals as recommended by the National Institutes of Health (NIH) and the Brazilian Society of Experimental Biology. All protocols were previously approved by the Ethics, Bioethics and Animal Welfare Committee of Vila Velha University (EBAW-UVV # 403/2016).

2.2. Treatments and experimental protocol (induction of CIN)

Mice were randomly divided into six groups as follows: group 1, control; group 2, contrast-induced nephropathy (CIN); rats administered with *N*-acetylcysteine (NAC, 200 mg/kg, group 3), with silymarin 50 mg/kg (S50, group 4), silymarin 200 mg/kg (S200, group 5) or silymarin 300 mg/kg (S300, group 6). Silymarin was obtained from Sigma-Aldrich (#S0292, St. Louis, MO, USA), and the doses were chosen based on previous studies in similar experimental animal models [18–21]. After five days of oral pretreatment with vehicle (groups 1 and 2), NAC (group 3) and silymarin (S50, S200 and S300), the CIN procedure was performed.

The CIN procedure in Swiss mice was performed according to previous protocols developed in our laboratory [1,4] adapted originally from Lee et al. [22] and Billings et al. [12] with minor modifications. Briefly, after overnight water deprivation (16 h), nitric oxide (NO) blockade and inhibition of prostaglandin synthesis, the mice were injected intraperitoneally (i.p.) with a low-osmolar monomeric iodinated radiocontrast medium, ioversol (Optiray, 320 Mallinckrodt Medical, Inc., St. Louis, MO, 1.5 g iodine/kg). For inhibition of NO synthase (NOS) and cyclooxygenase (COX), the mice were exposed to L-NG-nitro arginine methyl ester (L-NAME, 10 mg/kg i.p., diluted in 0.9% saline, Sigma Chemicals, St Louis, MO, USA) and indomethacin (10 mg/kg i.p, diluted in dimethylsulfoxide), respectively, 15 min before the ioversol injection. After the ioversol injection, the animals had free access to food and water. The animals were euthanized 24 h later using an overdose of sodium thiopental (Cristalia, Sao Paulo, Brazil, 200 mg/kg, i.p.) for biochemical and cyto-histopathological investigations.

2.3. Blood and kidney samples

Venous blood was collected from the right ventricle of animals euthanized with sodium thiopental (200 mg/kg, i.p.) and flushed through a syringe with EDTA (0.3 mol/L). Next, the blood was centrifuged at 4000 ×*g* for 10 min. Then, the serum was separated and stored at 4 °C until analysis. The serum concentrations of creatinine and urea nitrogen were determined using the Jaffe [23] and urease-indophenol methods [24], respectively. The serum concentration of cystatin C was measured using the turbidimetric method [25]. All measurements were obtained using an automatic biochemical analyzer (AU 400 or 680, Olympus/Beckman Coulter, Munich, Germany) from a clinical analysis laboratory (Tommasi Laboratory, Vitoria, ES, Brazil). Standard controls were run before each determination.

Immediately after perfusion of tissues with cold phosphate-buffered saline (PBS, pH 7.4, 0.1 mol/L) through the left ventricle, both kidneys were excised. Renal cells were prepared for flow cytometry analysis, based on previous and standardized studies in our laboratory [1,10,26,27]. Briefly, the tissues were grossly minced using surgical scissors and were incubated with an isolation solution containing trypsin (Sigma-Aldrich) to dissociate the cells. Next, the cell suspension was filtered through a nylon screen (BD, Becton Dickinson, San Jose, CA, USA, Falcon 70 μm) to remove the cellular debris. Finally, the samples were washed twice in PBS and stored at −80 °C until further analysis. For histopathological examination, kidney samples were fixed in paraformaldehyde (4%), and histological slides were prepared and counterstained with hematoxylin and eosin (HE).

2.4. Measurement of oxidative stress (ROS production) in the blood and kidney

The ROS availability was analyzed using flow cytometry. To estimate the intracellular superoxide ($\cdot O_2^-$) or hydrogen peroxide (H_2O_2) concentration, dihydroethidium (DHE, 160 μmol/L) and 2′,7′-dichlorofluorescein diacetate (DCF, 20 mmol/L) were added to the cell suspension (10^6 cells) and incubated at 37 °C for 30 min in the dark. Highly reactive oxygen species (hROS), such as hydroxyl radicals and peroxynitrite ($\cdot OH^-$/$ONOO^-$), were selectively detected by 2-[6-(4′-hydroxy)phenoxy-3H-xanthen-3-on-9-yl]benzoic acid (HPF, 10 μmol/L) as described by our group [1,10] and others [28]. The cells were then washed, resuspended in PBS and analyzed using the same flow cytometer (FACSCanto II, BD). All data were obtained using FACSDiva software (BD), and overlay histograms were analyzed using FCS Express trial software (De Novo). For quantification of DHE, DCF and HPF fluorescence, samples were acquired in duplicate, and 10,000 events were used for each measurement. The cells were excited at 488 nm; DHE fluorescence was detected using a 585/42 nm bandpass filter, and DCF/HPF fluorescence was detected using a 530/30 nm bandpass filter. Finally, the data were expressed as median fluorescence intensity (MFI, in a.u.).

2.5. Advanced oxidation protein products (AOPP) in plasma

The analyses of AOPP were performed according to Witko-Sarsat et al. [29] and Coutinho et al. [30] using spectrophotometry with a microplate reader (Spectra-MAX-190, Molecular Devices, Sunnyvale, CA, USA). First, 40 μL of plasma (diluted at 1:10) was solubilized 1:5 in PBS or chloramine-T standard solutions (0 to 100 μmol/L). Then, the samples were placed in each well of a 96-well microtiter plate (Becton Dickinson Labware, Lincoln Park, NJ, USA), and 10 μL of 1.16 mol/L

potassium iodide (KI, Sigma-Aldrich) was added, followed by the addition of 20 μL of acetic acid. Finally, the absorbance of the reaction mixture was immediately acquired at 340 nm using a microplate reader against a blank containing 200 μL of PBS, 10 μL of KI and 20 μL of acetic acid. Finally, the AOPP was determined when the correlation coefficient was > 0.95. The concentrations of total protein were analyzed by Bradford assay [31] at a plasma dilution of 1:200 for each measurement and presented in μmol/mg.

2.6. Comet assay

DNA damage was assessed using an alkaline comet assay (single cell gel electrophoresis) based on Singh et al. [32] following minor adaptations established in our laboratory [33–35]. Briefly, histological slides were precoated with 1.5% normal melting point agarose. Subsequently, 2×10^4 blood cells were embedded in 110 μL of 1% low melting point agarose and spread on agarose-precoated slides. After gelling at 4 °C for 30 min, the slides were incubated in freshly prepared lysis solution (2500 mmol/L NaCl, 100 mmol/L EDTA, 10 mmol/L Tris, and 34 mmol/L N-Lauroylsarcosine sodium, adjusted to pH 10.0–10.5 using freshly added 1% Triton X-100 and 10% DMSO) for 1 h at 4 °C. Then, the slides were placed in an electrophoresis chamber filled with freshly prepared alkaline buffer (300 mmol/L NaOH and 1 mmol/L EDTA, pH > 13) for 40 min at 4 °C and electrophoresed at 300 mA and 32 V (1 V/cm) for 20 min. Next, the slides were neutralized with 0.4 mol/L Tris buffer (pH 7.5) for 5 min (3 times) and finally dried with cold pure methanol (−20 °C) for fixation. Migration of DNA fragments towards the anode creates a comet-shaped tail, which is visualized by staining with ethidium bromide (20 μg/mL, Sigma-Aldrich). Images were obtained at a magnification of 20× using a fluorescence optical microscope (Nikon Eclipse TI, Melville, NY, USA) equipped with excitation (420–490 nm) and barrier (520 nm) filters. The coded images were acquired using a CCD camera (Nikon) and analyzed with CASP 98beta software (public domain). Among several parameters provided by the program CASP, we used the percentage of DNA in the tail and the tail moment for analysis of DNA damage. The images of 50 randomly selected nucleoids from each sample were analyzed for each animal. During the image analysis, nucleoids without clearly identifiable heads, overlapping nucleoids or nucleoids containing an artifact were excluded as a quality control parameter.

2.7. Apoptosis

Apoptotic kidney cells were quantified by annexin V-FITC and PI double staining using an annexin V-FITC apoptosis detection kit (BD), as previously described [1,36]. Briefly, renal cells were washed twice with PBS and adjusted to 500 μL of the binding buffer (5×10^5 cells). Then, the cell suspensions were incubated with annexin V-FITC and PI for 15 min at room temperature (25 °C) in the dark. Finally, the cells were analyzed with a FACSCanto II (BD) flow cytometer. Viable cells with positive staining for annexin V (Q2 + Q4) were considered apoptotic cells.

2.8. Cell viability

In accordance with previous studies from our laboratory, cell viability was analyzed using propidium iodide (PI) staining exclusion [1,26,36]. A total of 10^6 cells were incubated with 2 μL of PI for 5 min in the dark at ~23 °C. Then, the cells were washed with PBS and analyzed using a flow cytometer (FACSCanto II, BD Biosciences, San Jose, CA). For cell viability quantification, samples were acquired in triplicate, and 10,000 events were used for each measurement. The cells were excited at 488 nm, and PI fluorescence was detected using a 585/42 nm bandpass filter. The data are expressed as the percentage of unstained/viable cells [1].

2.9. Kidney histology

The renal tissues were embedded in paraffin, and sections (3.5 μm) were stained with HE. Tubulointerstitial injury (TILI), which is characterized by tubular atrophy, thickening of the basement membrane, dilatation and protein cast, was assessed by semiquantitative analysis in accordance with Bôa et al. [1]. First, twenty fields from each animal were examined at 400× magnification and graded according to a scale from 0 to 4 as follows: Grade 0, no tubulointerstitial injury; Grade 1, < 25% of the tubulointerstitium was injured; Grade 2, 25–50% of the tubulointerstitium was injured; Grade 3, 51–75% of the tubulointerstitium was injured; and Grade 4, 76–100% of the tubulointerstitium was injured. The TILI index was calculated by multiplying the number of fields with a sclerosis score of 1 by one, the number of fields with a score of 2 by two, the number of fields with a score of 3 by three, and the number of fields with a score of 4 by four. Finally, these values were summed and divided by the number of 20 fields assessed, including those with a sclerosis score of zero. All sections were examined by researchers blinded to the experimental groups of the samples.

2.10. Scanning electron microscopy (SEM)

Kidney samples from different groups were fixed in paraformaldehyde (4%) and refrigerated until the analysis. Longitudinal sections were cut with razor blade to divide the samples for SEM (scanning electron microscopy) and OM (optical microscopy). Next, each sample was washed 3 times with cacodylate buffer (0.1 M; pH 7.2) for 30 min each, postfixed in a solution of 1% osmium tetroxide (OsO_4) and 1.25% potassium ferrocyanide for 1 h at room temperature and protected from light. Then, the longitudinal sections of kidney samples were washed in cacodylate buffer and ultrapure water, dehydrated in ascending grades of ethanol (30%, 50%, 70%, 90% and 100%) for 30 min each, subjected to critical point drying in CO_2 (Autosandri-815, Tousimis), coated with 10 nm of pure gold in a vacuum sputter coater (Desk V, Denton Vacuum) and studied using a scanning electron microscope (JEOL, JEM6610 LV) in direct mode.

2.11. Statistical analysis

All data are expressed as the mean ± standard error mean (SEM). The flow cytometry data for ROS availability are expressed as the median coefficient of two repeated and statistically reproducible measurements of at least 5 independent animals (the Friedman test). Statistical analysis was performed by one-way analysis of variance (ANOVA) using Prism software (Prism 6.0, GraphPad Software, Inc., San Diego, CA, USA). Tukey's test was used for post hoc analysis when ANOVA showed significant differences. The differences were considered significant at $p < 0.05$.

3. Results

3.1. Silymarin attenuates renal dysfunction after CIN in mice

Fig. 1 summarizes the mean values of the main serum parameters used to estimate renal function. As expected, the CIN group exhibited a significant increase in urea (3.7-fold), creatinine (2.1-fold) and cystatin C (1.8-fold) compared with the control animals (51 ± 4 mg/dL, 0.26 ± 0.01 mg/dL and 0.26 ± 0.01 mg/L, respectively, $p < 0.05$). In relation to conventional treatment in clinical practice, the NAC group did not reduce any renal biomarkers (urea: 180 ± 15 mg/dL; creatinine: 0.48 ± 0.1 mg/dL and cystatin C: 0.73 ± 0.12 mg/L). Interestingly, all doses of silymarin were capable of preventing renal injury by CM ($p < 0.05$), as observed by the reduction of serum levels of urea (S50: 108 ± 26 mg/dL; S200: 102 ± 13 mg/dL and S300: 98 ± 15 mg/dL, $p < 0.05$), creatinine (S50: 0.21 ± 0.02 mg/dL; S200: 0.33 ± 0.02 mg/dL and S300: 0.3 ± 0.02 mg/dL, $p < 0.05$)

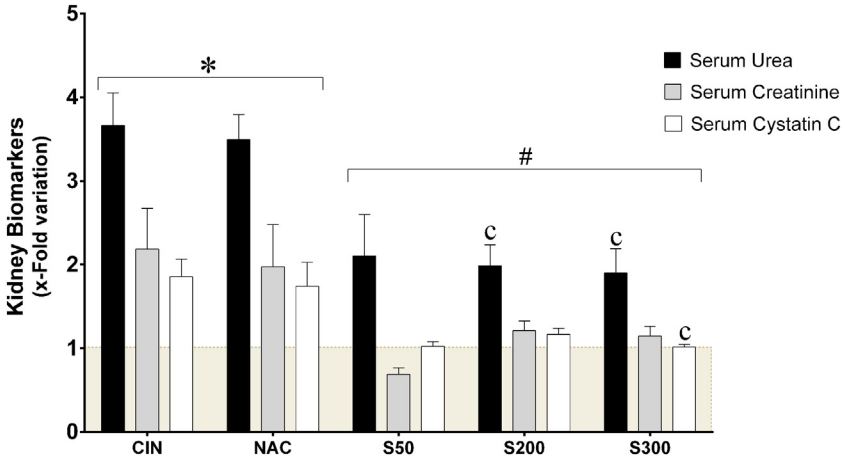

Fig. 1. The renoprotective effects of silymarin against radiocontrast-induced nephropathy in Swiss mice. Bar graph showing the average values of the main biomarkers of kidney function. The CIN group showed remarkably augmented levels of serum urea, creatinine and cystatin C. Unlike the NAC group, silymarin dose-dependently decreased these biomarkers (50, 200 and 300 mg/kg). Values are presented as the mean ± SEM for n = 6–12 animals per group. * $p < 0.05$ compared with the control group; # $p < 0.05$ compared with the CIN group; c $p < 0.05$ compared with the NAC group (one-way ANOVA).

and cystatin C (S50: 0.43 ± 0.02 mg/L; S200: 0.49 ± 0.03 mg/L and S300: 0.43 ± 0.01 mg/L, $p < 0.05$) compared with the CIN group. More specifically, only the S300 group showed a significant reduction in urea and cystatin C compared with the NAC group ($p < 0.05$).

3.2. Silymarin prevents blood oxidative stress after CIN in mice

To quantify the production of $\cdot O_2^-$, H_2O_2 and $\cdot OH^-/ONOO^-$ in white blood cells, we used flow cytometry with DHE, DCF and HPF indicators (respectively) in all groups studied. As summarized in the bar graphs in Fig. 2A, we observed an increase in blood ROS production in the CIN group (DHE: 39%; DCF: 21%; and HPF: 36%) compared with the control mice (DHE: 1540 ± 120 a.u.; DCF: 691 ± 38 a.u.; and HPF: 465 ± 60 a.u., $p < 0.05$). Furthermore, all treatments (NAC and all doses of silymarin administered) prevented the increase of serum bioavailability of $\cdot O_2^-$ (NAC: 1619 ± 47 a.u.; S50: 1523 ± 15 a.u.; S200: 1614 ± 32 a.u.; and S300: 1535 ± 10 a.u., $p < 0.05$), H_2O_2 (NAC: 672 ± 17 a.u.; S50: 677 ± 15 a.u.; S200: 701 ± 34 a.u.; and S300: 709 ± 27 a.u., $p < 0.05$) and $\cdot OH^-/ONOO^-$, (NAC: 401 ± 13 a.u.; S50: 393 ± 4 a.u.; S200: 386 ± 5 a.u.; and S300:

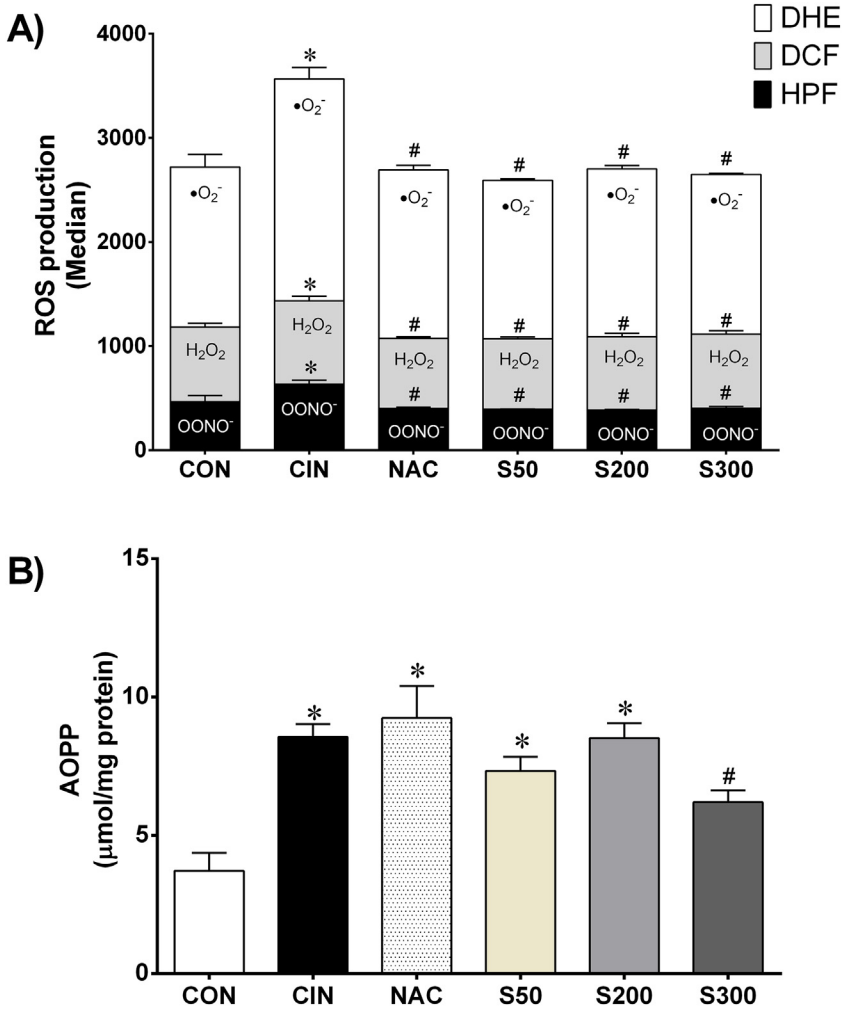

Fig. 2. Silymarin prevents blood oxidative stress against radiocontrast-induced nephropathy in Swiss mice. A) Blood ROS production was assessed by DHE, DCF and HPF as measured by flow cytometry. Bar graphs showing that after CIN, the white blood cells overproduced ROS, whereas NAC and all tested doses of silymarin prevented this effect. B) Quantification of serum protein oxidation (AOPP), in which only silymarin at the highest dose showed antioxidant effects. Values are presented as the mean ± SEM for n = 7–9 animals per group. *$p < 0.05$ compared with the control group and #$p < 0.05$ compared with the CIN group (one-way ANOVA).

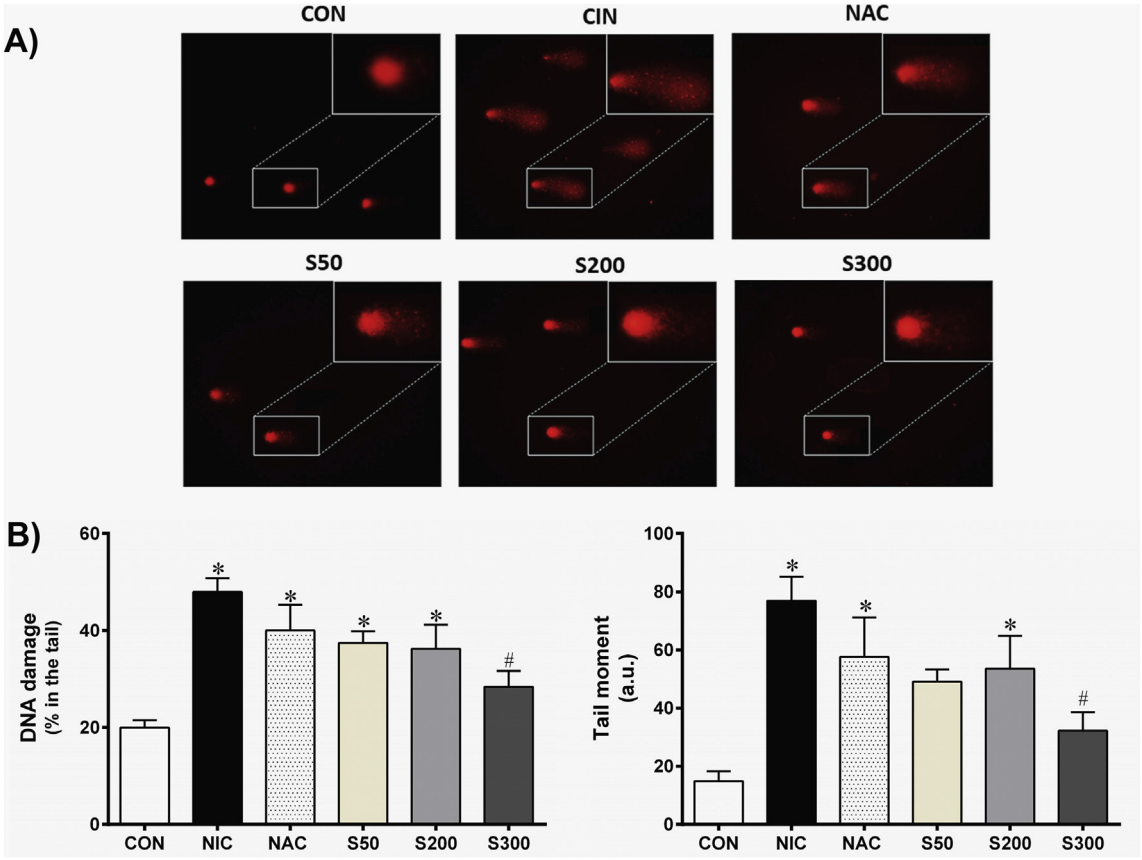

Fig. 3. A high dose of silymarin prevents DNA damage against radiocontrast-induced nephropathy in Swiss mice. A) Typical comets showing higher DNA fragmentation in the CIN group compared to the control group, in contrast with the S300 group. The comets were quantified and are shown in graphs in the bottom panel. B) Bar graphs showing the mean percentage of DNA damage and tail moment (~2.5-fold higher in the CIN group). Only S300 was able to protect the DNA of blood cells. Values are presented as the mean ± SEM for n = 5–6 animals per group. *p < 0.05 compared with the CON group and #p < 0.05 compared with the CIN group (one-way ANOVA).

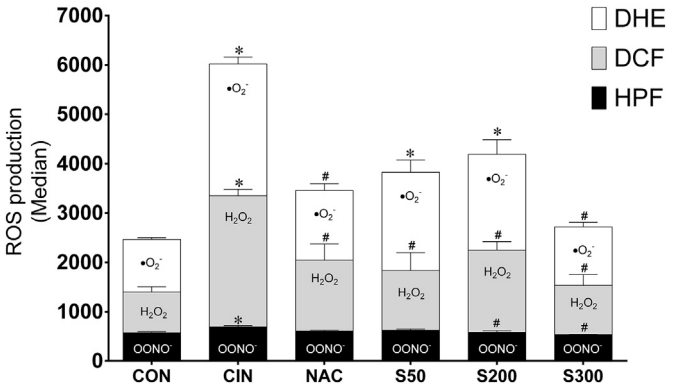

Fig. 4. Silymarin prevents renal ROS production against radiocontrast-induced nephropathy in Swiss mice. Bar graphs showing severe ROS overproduction in the CIN kidney, which was partially reversed by the NAC, S50 and S200 groups. Only silymarin at 300 mg/kg presents a reduction of $\cdot O_2^-$, H_2O_2 and $\cdot OH^-$/$ONOO^-$. Values are presented as the mean ± SEM for n = 5–6 animals per group. *p < 0.05 vs. control group and #p < 0.05 vs. CIN group (one-way ANOVA).

405 ± 17 a.u., p < 0.05) compared with the CIN group. As shown in Fig. 2B, the CIN group showed increased serum oxidized proteins compared with the control group (CIN: 8.6 ± 0.5 compared with CON: 3.7 ± 0.7 μmol/mg protein, p < 0.05). However, the standard treatment with NAC did not reduce AOPP serum levels (9.2 ± 1.1 μmol/mg protein, p > 0.05). In relation to the silymarin preventative strategy, only the highest dose was effective (S300: 6.2 ± 0.4 μmol/mg protein, p < 0.05).

3.3. Silymarin prevents blood DNA damage in the CIN model

As observed in Fig. 3A and B, the assessment of genotoxic stress by comet assay indicated higher DNA damage of blood cells in the CIN group (~2.5-fold) compared with the CON mice (20 ± 2%, p < 0.05). Among the preventative strategies, the conventional NAC and lower doses of silymarin were similar to the CIN group (NAC: 40 ± 5%; S50: 37 ± 2% and S200: 36 ± 5%, p > 0.05). Interestingly, only S300 was able to prevent DNA damage (28 ± 3%) compared with the CIN group (48 ± 3%, p < 0.05). Concerning the comet tail moment, including the product of the tail length and the portion of total DNA in the tail [33,35], there was a similar profile of the first analysis (Fig. 3A); an increase in DNA fragmentation in the CIN group (77 ± 8 a.u.) compared with the CON group (15 ± 3 a.u., p < 0.05). Only the highest dose of silymarin reduced this parameter (32 ± 6 a.u., p < 0.05) compared with other groups (NAC: 58 ± 14 a.u.; S50: 49 ± 4 a.u. and S200: 54 ± 11 a.u., p > 0.05).

3.4. Silymarin prevents renal oxidative stress after CIN in mice

We also investigated the impact of CIN on oxidative damage in kidney tissues from all groups using the same ROS indicators. Similar to the observations in the blood, Fig. 4 shows severe ROS overproduction in CIN kidneys (DHE: 151%; DCF: 220%; and HPF: 21%) compared with control mice (DHE: 1064 ± 33 a.u.; DCF: 830 ± 107 a.u.; and HPF: 571 ± 23 a.u., p < 0.05). However, the conventional prevention with

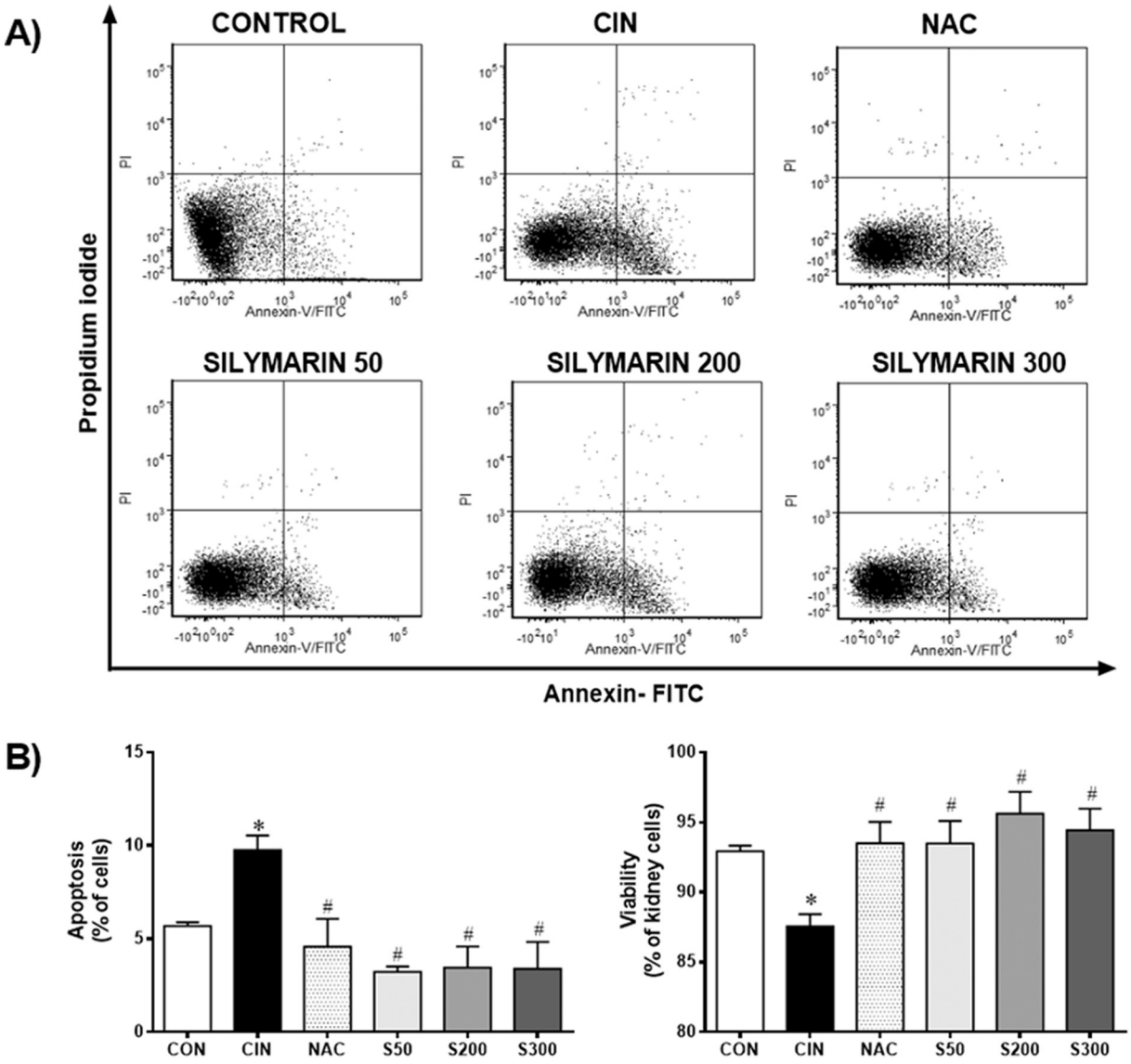

Fig. 5. Silymarin prevents apoptosis and restores renal cell viability after CIN in Swiss mice. A) Dot plots showing the increase in apoptosis in CIN animals compared with all treated groups, determined through propidium iodide (PI) and annexin V-FITC staining. B) Bar graphs showing the apoptotic indices (Q2 + Q4) of all groups (left panel) and the renal cell viability highlighting the increase in CIN and the prevention with NAC and silymarin (50, 200 and 300 mg/kg) (right panel). Values are presented as the mean ± SEM for n = 5–7 animals per group. *p < 0.05 compared with the control group and #p < 0.05 compared with the CIN group (one-way ANOVA).

NAC inhibited the increase in the renal levels of only $\cdot O_2^-$ and H_2O_2 (1417 ± 136 and 1435 ± 328 a.u., respectively, p < 0.05) compared with the CIN mice. Interestingly, silymarin showed a dose-dependent decrease in oxidative stress, reducing it significantly according to the three ROS biomarkers at the highest dose (DHE: 1187 ± 92 a.u.; DCF: 998 ± 221 a.u.; and HPF: 535 ± 6 a.u., p < 0.05) compared with the CIN group.

3.5. Apoptosis and cell viability

Apoptosis was evaluated in the same kidney cells using PI and annexin V staining followed by flow cytometry analysis, which is one of the best methods for this purpose. Fig. 5A shows representative dot plots for each group. We observed a notable increase in the number of apoptotic cells (Q2 + Q4) in the CIN group (~1.7-fold) compared with the control mice (5.7 ± 0.2%, p < 0.05), as shown in Fig. 5B (left panel). Interestingly, all treatments (NAC and all doses of silymarin) prevented the increase in apoptosis (NAC: 4.6 ± 1.5%; S50: 3.2 ± 0.3%; S200: 3.4 ± 1.1%; and S300: 3.4 ± 1.4%, p < 0.05) compared with the CIN group (p < 0.05). Concerning cell viability (Fig. 5B, right panel), the CIN group impaired cell viability (87.6 ± 0.9%) compared with all treated groups (NAC: 93.5 ± 1.5%; S50: 93.5 ± 1.6%; S200: 95.6 ± 1.6%; and S300: 94.4 ± 1.5%, p < 0.05).

3.6. Kidney morphometric parameters

As shown in Fig. 6, histological analysis showed that the CIN group exhibited remarkable damages in the renal microarchitecture (Fig. 6, top panel). The CIN group showed increased glomerular damage, loss of nuclei, tubular dilation with luminal congestion, tubular epithelial cell vacuolization, tubular shedding and more tubulointerstitial lesions compared with the control mice (CIN: 3.49 ± 0.11 compared with CON: 0.05 ± 0.01, p < 0.05) (Fig. 6, bottom panel). Interestingly, the conventional treatment with NAC and all tested doses of silymarin reduced these lesions (NAC: 57%; S50: 30%; S200: 64% and S300: 62%,

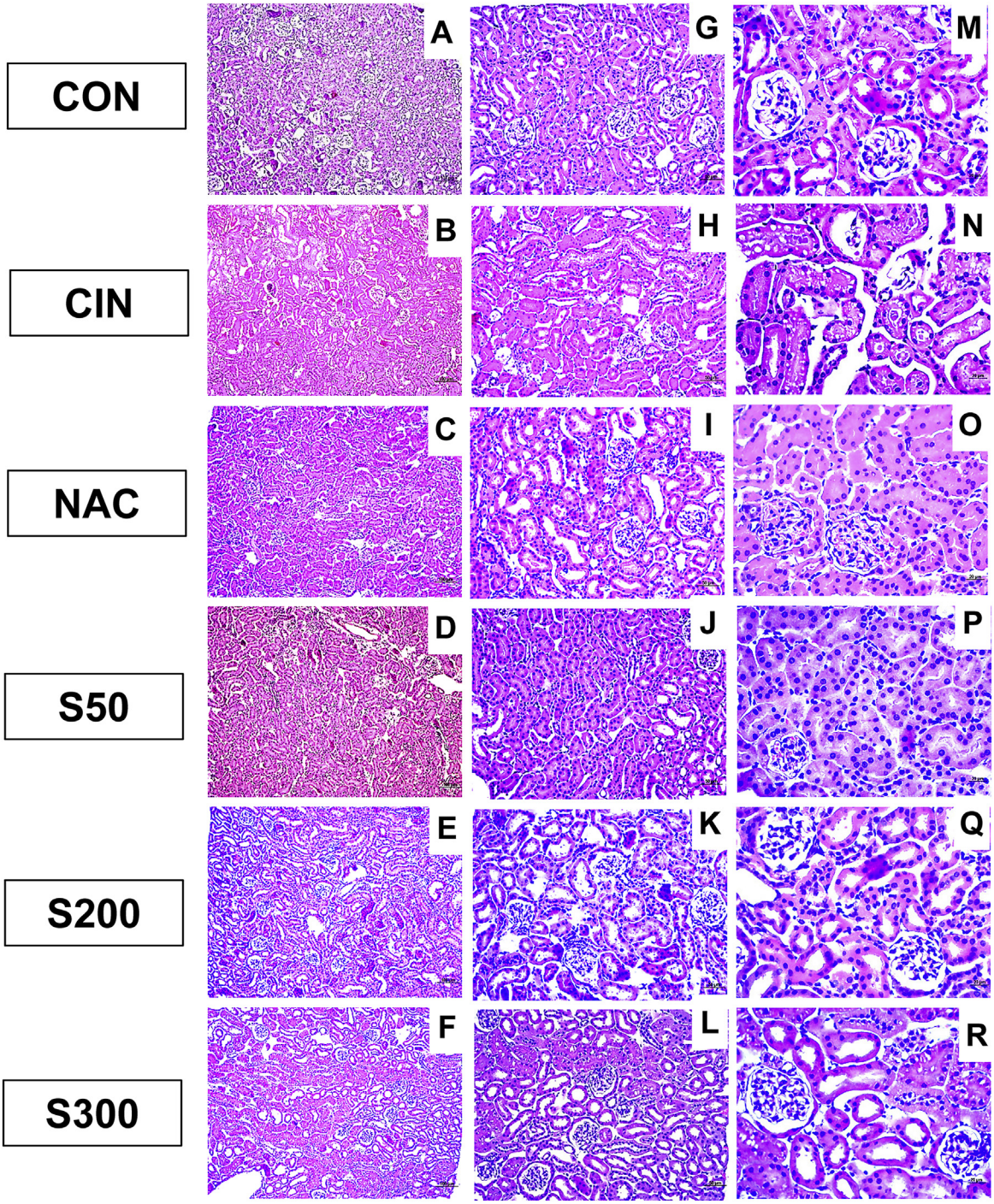

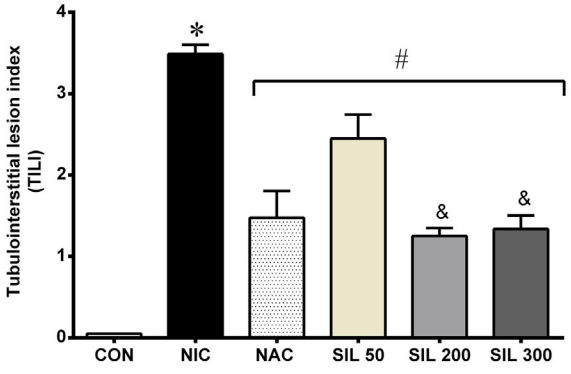

(caption on next page)

Fig. 6. TILI index. Silymarin ameliorates glomerular and tubulointerstitial lesions in radiocontrast-induced nephropathy in mice. Top panel: Representative micrographs showing kidney histology (stained with hematoxylin and eosin) in different groups of mice 24 h after induction of CIN. A–F: The cortex-medulla section (100×); G–L: the cortical region (200×) and M–R: the cortical region (400×), showing glomerular damage, loss of nuclei, increased luminal congestion, epithelial cell shedding, tubular dilation and tubulointerstitial lesions mainly in the CIN group, which was prevented in a dose-dependent manner with silymarin. Bottom panel: The tubulointerstitial lesion (TILI) indices of all groups (n = 4). The values are presented as the mean ± SEM. *p < 0.05 compared with the control group.

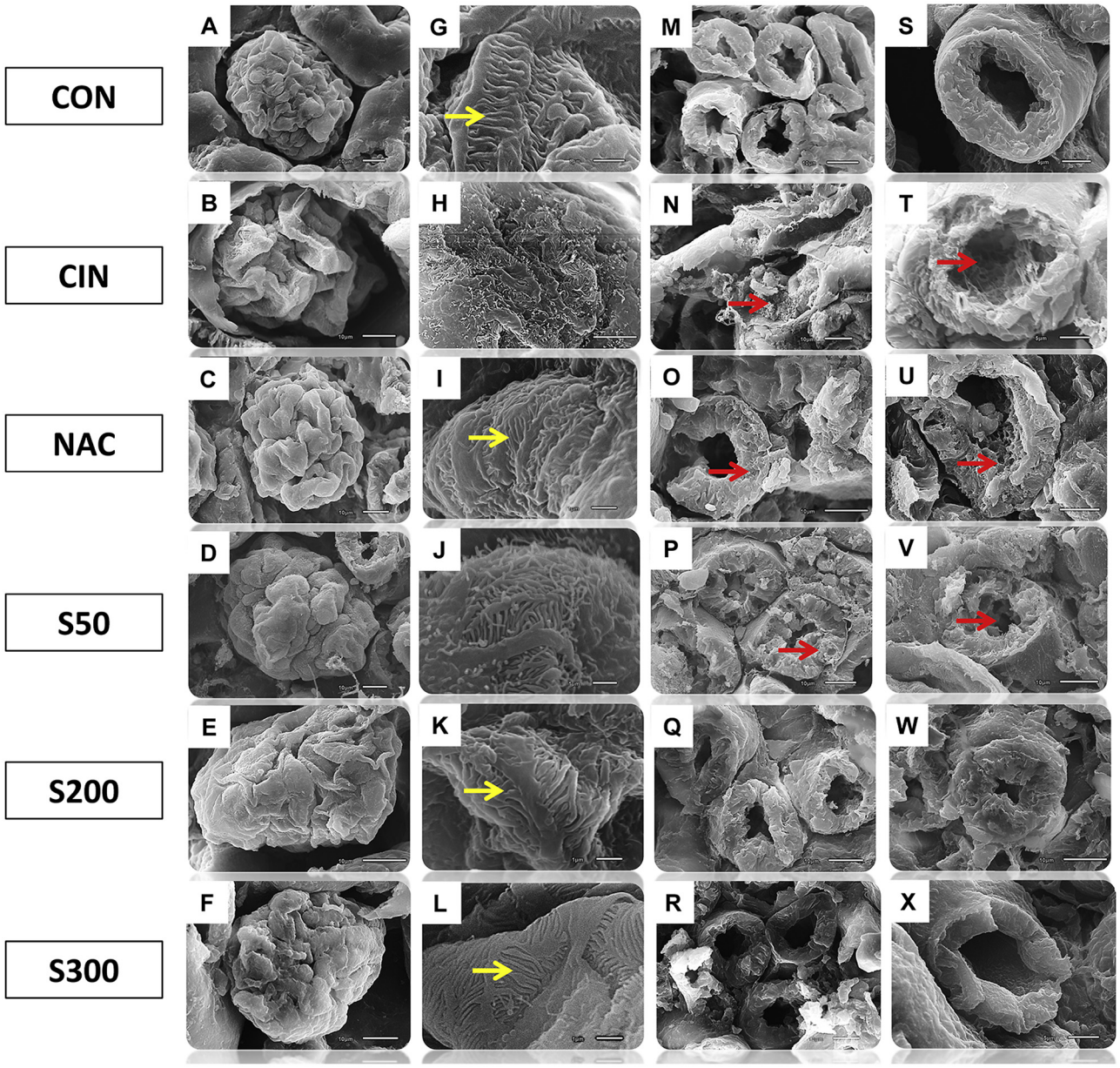

Fig. 7. Scanning electron microscopy (SEM) images. Kidney tissue samples from different groups confirmed the decrease in renal glomerular and tubular injuries. The first column (A–F, scale bar = 10 μm) shows SEM images of whole glomeruli, showing greater structural preservation of the surface tissues in the NAC (C) and S300 (F) groups, similar to the control group. The CIN (B), S50 (D) and S200 (E) groups exhibited a loss of structural cohesion. The second column (G–L, scale bar = 1 μm) shows higher magnification of podocytes to show the primary processes and the interdigitating secondary processes. The CIN (B) and S50 (D) groups showed atypical podocytes. Only the NAC (I), S200 (K) and S300 (L) groups were similar to the control structures (G), with smooth foot processes that tightly apposed each other (yellow arrows). The third column (M–R, scale bar = 10 μm) shows SEM images of proximal tubules with normal structure (M), with cell epithelial vacuolization (red arrows) after radiocontrast nephropathy (N, O and P) and the absence of cytoplasmic vacuoles in the S200 (Q) and S300 (R) groups. The last column (S–X, scale bar = 5 or 10 μm) shows more details of tubular structure according to the response pattern shown in the third column, emphasizing a dose-dependent protective effect of silymarin. (For interpretation of the references to color in this figure legend, the reader is referred to the web version of this article.)

$p < 0.05$) compared with the CIN group. Among these preventative treatments, only the lowest dose of silymarin S50 was less effective than the others (NAC, S200 and S300, $p < 0.05$).

Fig. 7 shows typical SEM photomicrographs confirming the results obtained in our previously mentioned results. In the CIN group, we observed a shrunken glomerular tuft (Fig. 7B), loss of structural cohesion with atypical podocytes (Fig. 7H), luminal congestion and vacuolization of tubular epithelial cells (Fig. 7, images N and T) compared to the control group. Interestingly, the NAC (Fig. 7, images C, I, O and U), S200 (Fig. 7, images E, K, Q, and W) and S300 (Fig. 7, images F, L, R

and X) groups prevented iodinated contrast-induced lesions in both glomerular podocytes and tubular cells.

4. Discussion

Although recent studies have suggested the efficacy of silymarin for some renal diseases, such as diabetic nephropathy [37,38] or iatrogenic nephrotoxicity induced by therapeutic drugs [39,40], the efficacy of silymarin in preventing contrast-induced renal dysfunction remains inconclusive [5]. To the best of our knowledge, our study is the first to demonstrate experimentally that silymarin (including a low dose of 50 mg/kg) is able to prevent the development of CIN by preserving renal function, reducing blood and renal oxidative stress/apoptosis, increasing renal cell viability and attenuating the incidences of renal glomerular and tubular injuries, as shown by the histological analysis.

Although the first clinical case of contrast-impaired renal injury was reported in 1942 [2,41], the first experimental model appeared only in the 1980s in rabbits and rats [42] and presented some variations over time (e.g., animal model, type of contrast agent, dehydration and/or different combinations of drug injuries). In 2015, our laboratory successfully developed a novel, simple and reproducible CIN experimental model in Swiss mice by administering the contrast agent intraperitoneally [1], differing from the majority of previous murine studies that administered contrast agents intravascularly [12,43]. In addition, because the injection of contrast agent alone does not cause overt acute kidney injury in rodents (nor in healthy patients), we maintained the use of prostaglandin and NO inhibitors in accordance with previous studies [2,3,12,22]. Therefore, this adjuvant pharmacological strategy mimics the clinical conditions that usually predispose an atherosclerotic patient to CIN (elderly and hypertensive/diabetic patients), resulting in a decline in renal function [1,2].

In recent years, some researchers have argued that the future gold standard in CIN diagnostics must be determined in a synergistic approach that includes different biomarkers and functional imaging techniques [2,44,45]. Therefore, to increase the reliability of renal impairment in the present study, we have incorporated some analysis, starting with the serum cystatin C measurement. As this peptide increases proportionally to the decrease in the glomerular filtration rate and shows a small volume of distribution, it has recently been considered an important endogenous biomarker of acute kidney injury [25,45–47]. According to our hypothesis, the increase in all three renal biomarkers (urea, creatinine and cystatin C) in the CIN group confirms the success of acute nephropathy but fortunately, not in the CIN groups treated with silymarin at all doses studied. In addition, our negative data in the NAC group notably corroborate recent studies that challenge the utility of this inexpensive and safe antioxidant for the prevention of CIN in clinical practice [7,9,45,48]. More interestingly, we also observed that the attenuation of uremia and cystatin C in the S300 group was significant compared with the NAC group ($p < 0.05$), demonstrating an important potential role for silymarin in protecting against contrast-induced renal injury. Considering that oxidative damage is one of the main pathogenic mechanisms involved in CIN [1,9,47,48] and that silymarin displays high antioxidant properties [14,16,17], we also extended this investigation to oxidative stress-related parameters in the blood and kidneys of all groups, as discussed below.

Among the studies involving CIN, the uncommon investigation of systemic extrarenal adverse effects has been evidenced only by indirect methods of oxidative stress both in animals [49–51] and humans [52]. For the first time, it was demonstrated that both direct (ROS detection) and indirect methods (AOPP and comet assay) detected iodinated contrast increases in blood (systemic) oxidative stress in the same animals. More interestingly, conventional NAC and silymarin prevention can reverse blood ROS overproduction. Regarding protein oxidation and DNA damage, better prevention may be achieved with the highest dose of silymarin (but not by NAC), as observed in biomarkers of renal function. This apparent difference between methods may be partially explained by a faster ROS washout compared with the analysis of cumulatively oxidized macromolecules [1]. Furthermore, it emphasizes the importance of analyzing different tests of oxidative damage, since they might provide additional oxidative stress data. For example, since serum AOPP biomarkers may be related to the progression of renal failure [29,53,54], we included this analysis in our investigation. Our hypothesis is that the reduction in uremia and improvement in ROS status in the kidney may be related to AOPP serum reduction, as observed by others [53,55].

Concerning renal toxicity, we also observed that silymarin inhibits ROS overproduction in a dose-dependent manner. Since it is known that the oxidative damage has major consequences, such as elevation of apoptosis and decrease in cell viability through established pathways (e.g., activation of caspases, telomere shortening, and/or chromosomal cleavages) [1,34,35,56], we investigated whether silymarin could also decrease these parameters, even under exposure to an iodinated contrast agent. The present data suggest that the slight modification of the lower dose of silymarin can provide antiapoptotic effects and improve renal cell viability, as well as the standard NAC. These anti-ROS and cell-protective processes observed for silymarin may be supported by some interrelating mechanisms recently described in other models of nephropathy as follows: scavenging activity [39], metal chelation [16,57], increased activity of antioxidative enzymes [58], repair and removal of damaged molecules [16] and/or mitochondrial protection [59].

In addition to the biochemical and flow cytometric analysis, our histological and scanning electron microscope examinations showed a pronounced disruption of renal ultrastructure in the CIN group compared with the control mice, consistent with previous reports from our group [1,4] and other groups [12,51,60,61]. In relation to silymarin intervention, another novelty of this study is the nephroprotective effect, which ameliorates glomeruli and tubular structures in a dose-dependent manner.

Regarding the set doses of silymarin, which are apparently high, it is important that the animal dose should not be extrapolated to a human equivalent dose by a simple conversion based on body weight, which has frequently been reported by some investigators [62,63]. Attempting to optimize this conversion of drug doses from animal experimental studies to future clinical trials, some investigators have suggested a simple method of using the body surface area normalization method [64,65]. After applying those calculations, we noted that all doses chosen in this study (50, 200 and 300 mg/kg) may be compatible with those used in humans (4, 16 and 24 mg/kg, respectively). As an extreme example, for a human weighing 85 kg, an oral administration of 2040 mg/day would be safe and well tolerated, as observed by others [14,66]. Therefore, the dose of silymarin used in the present study could be compatible with that being proposed in future clinical trials. In addition, since this flavonoid mixture has shown safety and efficacy profiles of usage in previous studies conducted in both animals and humans, we hope that further trials with large sample sizes, distinct dosages and durations are conducted against CIN. Furthermore, our findings provide new insights to investigate the role of silymarin in other experimental models of nephropathy induced by other pro-oxidant substances such as nandrolone [67] or acetylcholinesterase inhibitors (insecticides) [68].

A limitation of the study is that we did not analyze other renal parameters, such as proteinuria, which is a potential biomarker for tubular damage and impaired renal function. Moreover, in future studies, we intend to investigate the effects of silymarin on renal hemodynamic parameters in this experimental Swiss mouse model of CIN (recently developed in our laboratory). These data can be obtained by measuring inulin and sodium paraaminohippurate clearance to estimate the glomerular filtration rate and renal plasma flow, respectively [10].

5. Conclusion

In summary, the present study demonstrates for the first time that silymarin decreases systemic and renal oxidative damage, preserving renal function and morphological architecture under exposure to a radiocontrast agent in mice. More specifically, this renoprotective role is accompanied by antigenotoxic and antiapoptotic activities. Therefore, this flavonoid mixture may have promising clinical applications against CIN.

Financial support

This work was financially supported by grants from the National Council for the Development of Science and Technology (CNPq, 445080/2014-0 and 445736/2014-3) and the State Agency for the Development of Science and Technology (FAPES-74417495/16; 403/2016; 239/2016; 0606/2015).

Disclosure of interest

The authors declare that they have no conflict of interest.

Acknowledgements

The authors thank the Tommasi Laboratory for analysis and for use of their facilities and the Laboratory of Cellular Ultrastructure Carlos Alberto Redins (LUCCAR) for technical assistance and use of the microscope.

References

[1] I.S.F. Bôa, M.L. Porto, A.C.H. Pereira, J.P.L. Ramos, R. Scherer, J.P. Oliveira, B.V. Nogueira, S.S. Meyrelles, E.C. Vasquez, D.C. Endringer, T.M.C. Pereira, Resin from Virola oleifera protects against radiocontrast-induced nephropathy in mice, PLoS One 10 (2015) 1–15, https://doi.org/10.1371/journal.pone.0144329.

[2] N. Kiss, P. Hamar, Histopathological evaluation of contrast-induced acute kidney injury rodent models, Biomed. Res. Int. 2016 (2016) 3763250, , https://doi.org/10.1155/2016/3763250.

[3] C. Mamoulakis, K. Tsarouhas, I. Fragkiadoulaki, I. Heretis, M.F. Wilks, D.A. Spandidos, C. Tsitsimpikou, A. Tsatsakis, Contrast-induced nephropathy: basic concepts, pathophysiological implications and prevention strategies, Pharmacol. Ther. 180 (2017) 99–112, https://doi.org/10.1016/j.pharmthera.2017.06.009.

[4] K.L. Guss, S. Pavanni, B. Prati, L. Dazzi, J.P. de Oliveira, B.V. Nogueira, T.M.C. Pereira, M. Fronza, D.C. Endringer, R. Scherer, Ultrasound-assisted extraction of Achyrocline satureioides prevents contrast-induced nephropathy in mice, Ultrason. Sonochem. 37 (2017) 368–374, https://doi.org/10.1016/j.ultsonch.2017.01.035.

[5] Z. Sedighifard, F. Roghani, P. Bidram, S.A. Harandi, S. Molavi, Silymarin for the prevention of contrast-induced nephropathy: a placebo-controlled clinical trial, International Journal of Preventive Medicine. January-20 (2016). doi:https://doi.org/10.4103/2008-7802.174762.

[6] W.-Q. Ma, Y. Zhao, Y. Wang, X.-Q. Han, Y. Zhu, N.-F. Liu, Comparative efficacy of pharmacological interventions for contrast-induced nephropathy prevention after coronary angiography: a network meta-analysis from randomized trials, Int. Urol. Nephrol. (2018), https://doi.org/10.1007/s11255-018-1814-0.

[7] S.D. Weisbord, M. Gallagher, H. Jneid, S. Garcia, A. Cass, S.-S. Thwin, T.A. Conner, G.M. Chertow, D.L. Bhatt, K. Shunk, C.R. Parikh, E.O. McFalls, M. Brophy, R. Ferguson, H. Wu, M. Androsenko, J. Myles, J. Kaufman, P.M. Palevsky, PRESERVE trial group, outcomes after angiography with sodium bicarbonate and acetylcysteine, N. Engl. J. Med. 378 (2018) 603–614, https://doi.org/10.1056/NEJMoa1710933.

[8] T. Scharnweber, L. Alhilali, S. Fakhran, Contrast-induced acute kidney injury, Magn. Reson. Imaging Clin. N. Am. 25 (2017) 743–753, https://doi.org/10.1016/j.mric.2017.06.012.

[9] M.A. Hossain, E. Costanzo, J. Cosentino, C. Patel, H. Qaisar, V. Singh, T. Khan, J.S. Cheng, A. Asif, T.J. Vachharajani, Contrast-induced nephropathy: Pathophysiology, risk factors, and prevention, Saudi Journal of Kidney Diseases and Transplantation: An Official Publication of the Saudi Center for Organ Transplantation, Saudi Arabia, 29 (2018), pp. 1–9, https://doi.org/10.4103/1319-2442.225199.

[10] L.S. De Almeida, J.R. Barboza, F.P.S. Freitas, M.L. Porto, E.C. Vasquez, S.S. Meyrelles, A.L. Gava, T.M.C. Pereira, Sildenafil prevents renal dysfunction in contrast media-induced nephropathy in Wistar rats, Hum. Exp. Toxicol. 35 (2016) 1194–1202, https://doi.org/10.1177/0960327115626582.

[11] G. Efstratiadis, P. Pateinakis, G. Tambakoudis, A. Pantzaki, D. Economidou, D. Memmos, Contrast media-induced nephropathy: case report and review of the literature focusing on pathogenesis, Hippokratia. 12 (2008) 87–93 http://www.ncbi.nlm.nih.gov/pubmed/18923657.

[12] F.T. Billings, S.W.C. Chen, M. Kim, S.W. Park, J.H. Song, S. Wang, J. Herman, V. D'Agati, H.T. Lee, α2-Adrenergic agonists protect against radiocontrast-induced nephropathy in mice, American Journal of Physiology-Renal Physiology. 295 (2008) F741–F748. doi:https://doi.org/10.1152/ajprenal.90244.2008.

[13] M. Andreucci, T. Faga, R. Serra, G. De Sarro, A. Michael, Update on the renal toxicity of iodinated contrast drugs used in clinical medicine, Drug, Healthcare and Patient Safety. 9 (2017) 25–37, https://doi.org/10.2147/DHPS.S122207.

[14] S.J. Polyak, P. Ferenci, J.M. Pawlotsky, Hepatoprotective and antiviral functions of silymarin components in hepatitis C virus infection, Hepatology. 57 (2013) 1262–1271, https://doi.org/10.1002/hep.26179.

[15] L. Abenavoli, R. Capasso, N. Milic, F. Capasso, Milk thistle in liver diseases: past, present, future, Phytotherapy Research: PTR 24 (2010) 1423–1432, https://doi.org/10.1002/ptr.3207.

[16] P. Surai, Silymarin as a natural antioxidant: an overview of the current evidence and perspectives, Antioxidants. 4 (2015) 204–247, https://doi.org/10.3390/antiox4010204.

[17] A. Federico, M. Dallio, C. Loguercio, Silymarin/silybin and chronic liver disease: a marriage of many years, Molecules (Basel, Switzerland). 22 (2017), https://doi.org/10.3390/molecules22020191.

[18] J. Pérez-H, C. Carrillo-S, E. García, G. Ruiz-Mar, R. Pérez-Tamayo, A. Chavarría, Neuroprotective effect of silymarin in a MPTP mouse model of Parkinson's disease, Toxicology. 319 (2014) 38–43, https://doi.org/10.1016/j.tox.2014.02.009.

[19] J. Tan, J. Hu, Y. He, F. Cui, Protective role of silymarin in a mouse model of renal ischemia-reperfusion injury, Diagn. Pathol. 10 (2015) 198, https://doi.org/10.1186/s13000-015-0436-4.

[20] B.M. Razavi, G. Karimi, Protective effect of silymarin against chemical-induced cardiotoxicity, Iranian Journal of Basic Medical Sciences. 19 (2016) 916–923 http://www.ncbi.nlm.nih.gov/pubmed/27803777.

[21] R.J. Kate, R.M. Perez, D. Mazumdar, K.S. Pasupathy, V. Nilakantan, M. Luo, Y. Yang, J. Xu, W. Cheng, X.-W. Li, M.-M. Tang, H. Liu, F.-Y. Liu, S.-B. Duan, A new scoring model for the prediction of mortality in patients with acute kidney injury, BMC Medical Informatics and Decision Making. 7 (2017) 7862, https://doi.org/10.1186/s12911-016-0277-4.

[22] H.T. Lee, M. Jan, S.C. Bae, J.D. Joo, F.R. Goubaeva, J. Yang, M. Kim, A1 adenosine receptor knockout mice are protected against acute radiocontrast nephropathy in vivo, American Journal of Physiology. Renal Physiology. 290 (2006) F1367–F1375, https://doi.org/10.1152/ajprenal.00347.2005.

[23] G.R. Hervey, Determination of creatinine by the Jaffé reaction, Nature. 171 (1953) 1125 http://www.ncbi.nlm.nih.gov/pubmed/13072520.

[24] J.K. Fawcett, J.E. Scott, A rapid and precise method for the determination of urea, J. Clin. Pathol. 13 (1960) 156–159 http://www.ncbi.nlm.nih.gov/pubmed/13821779.

[25] D.M. Dalcomune, J. Terrão, M.L. Porto, E.C. Vasquez, M.P. Baldo, T.M.C. Pereira, Predictive value of cystatin C for the identification of illness severity in adult patients in a mixed intensive care unit, Clin. Biochem. 49 (2016) 762–767, https://doi.org/10.1016/j.clinbiochem.2016.04.004.

[26] I.B.S. Gomes, M.L. Porto, M.C.L.F.S. Santos, B.P. Campagnaro, T.M.C. Pereira, S.S. Meyrelles, E.C. Vasquez, Renoprotective, anti-oxidative and anti-apoptotic effects of oral low-dose quercetin in the C57BL/6J model of diabetic nephropathy, Lipids Health Dis. 13 (2014) 184, https://doi.org/10.1186/1476-511X-13-184.

[27] A.T. Dias, B.P. Rodrigues, M.L. Porto, A.L. Gava, C.M. Balarini, F.P.S. Freitas, Z. Palomino, D.E. Casarini, B.P. Campagnaro, T.M.C. Pereira, S.S. Meyrelles, E.C. Vasquez, Sildenafil ameliorates oxidative stress and DNA damage in the stenotic kidneys in mice with renovascular hypertension, J. Transl. Med. 12 (2014) 35, https://doi.org/10.1186/1479-5876-12-35.

[28] K. Setsukinai, Y. Urano, K. Kakinuma, H.J. Majima, T. Nagano, Development of novel fluorescence probes that can reliably detect reactive oxygen species and distinguish specific species, J. Biol. Chem. 278 (2003) 3170–3175, https://doi.org/10.1074/jbc.M209264200.

[29] V. Witko-Sarsat, M. Friedlander, C. Capeillère-Blandin, T. Nguyen-Khoa, A.T. Nguyen, J. Zingraff, P. Jungers, B. Descamps-Latscha, Advanced oxidation protein products as a novel marker of oxidative stress in uremia, Kidney Int. 49 (1996) 1304–1313 http://www.ncbi.nlm.nih.gov/pubmed/8731095.

[30] P.N. Coutinho, B.P. Pereira, A.C. Hertel Pereira, M.L. Porto, A.L.E. Monteiro de Assis, A. Côgo Destefani, S.S. Meyrelles, E.C. Vasquez, B.V. Nogueira, T.U. de Andrade, D.C. Endringer, M. Fronza, T.M. Costa Pereira, Chronic administration of antioxidant resin from Virola oleifera attenuates atherogenesis in LDLr −/− mice, J. Ethnopharmacol. 206 (2017) 65–72, https://doi.org/10.1016/j.jep.2017.05.015.

[31] M.M. Bradford, A rapid and sensitive method for the quantitation of microgram quantities of protein utilizing the principle of protein-dye binding, Anal. Biochem. 72 (1976) 248–254 http://www.ncbi.nlm.nih.gov/pubmed/942051.

[32] N.P. Singh, M.T. McCoy, R.R. Tice, E.L. Schneider, A simple technique for quantitation of low levels of DNA damage in individual cells, Exp. Cell Res. 175 (1988) 184–191 http://www.ncbi.nlm.nih.gov/pubmed/3345800.

[33] B.P. Rodrigues, B.P. Campagnaro, C.M. Balarini, T.M.C. Pereira, S.S. Meyrelles, E.C. Vasquez, Sildenafil ameliorates biomarkers of genotoxicity in an experimental model of spontaneous atherosclerosis, Lipids Health Dis. 12 (2013) 128, https://doi.org/10.1186/1476-511X-12-128.

[34] C.L. Tonini, B.P. Campagnaro, L.P.S. Louro, T.M.C. Pereira, E.C. Vasquez, S.S. Meyrelles, Effects of aging and hypercholesterolemia on oxidative stress and DNA damage in bone marrow mononuclear cells in apolipoprotein E-deficient mice, Int. J. Mol. Sci. 14 (2013) 3325–3342, https://doi.org/10.3390/ijms14023325.

[35] M.L. Porto, B.P. Rodrigues, T.N. Menezes, S.L. Ceschim, D.E. Casarini, A.L. Gava, T.M.C. Pereira, E.C. Vasquez, B.P. Campagnaro, S.S. Meyrelles, Reactive oxygen

species contribute to dysfunction of bone marrow hematopoietic stem cells in aged C57BL/6 J mice, J. Biomed. Sci. 22 (2015) 97, , https://doi.org/10.1186/s12929-015-0201-8.
[36] E. de A.O. Rua, M.L. Porto, J.P.L. Ramos, B.V. Nogueira, S.S. Meyrelles, E.C. Vasquez, T.C. Pereira, Effects of tobacco smoking during pregnancy on oxidative stress in the umbilical cord and mononuclear blood cells of neonates, J. Biomed. Sci. 21 (2014) 105, , https://doi.org/10.1186/s12929-014-0105-z.
[37] M.K. Fallahzadeh, B. Dormanesh, M.M. Sagheb, J. Roozbeh, G. Vessal, M. Pakfetrat, Y. Daneshbod, E. Kamali-Sarvestani, K.B. Lankarani, Effect of addition of silymarin to renin-angiotensin system inhibitors on proteinuria in type 2 diabetic patients with overt nephropathy: a randomized, double-blind, placebo-controlled trial, American Journal of Kidney Diseases: The Official Journal of the National Kidney Foundation. 60 (2012) 896–903, https://doi.org/10.1053/j.ajkd.2012.06.005.
[38] M. Rafieian-Kopaie, H. Nasri, Silymarin and diabetic nephropathy, Journal of Renal Injury Prevention. 1 (2012) 3–5, https://doi.org/10.12861/jrip.2012.02.
[39] C. Ninsontia, K. Pongjit, C. Chaotham, P. Chanvorachote, Silymarin selectively protects human renal cells from cisplatin-induced cell death, Pharm. Biol. 49 (2011) 1082–1090, https://doi.org/10.3109/13880209.2011.568506.
[40] F. Shahbazi, S. Dashti-Khavidaki, H. Khalili, M. Lessan-Pezeshki, Potential renoprotective effects of silymarin against nephrotoxic drugs: a review of literature, J. Pharm. Pharm. Sci. 15 (2012) 112–123, https://doi.org/10.18433/J3F88S.
[41] E. Pendergrass, G. Chamberlain, A survey of death and unfavorable sequelae following the administration of contrast media, American College of Radiology 48 (1942) 741–762.
[42] K. Golman, S. Holtås, Proteinuria produced by urographic contrast media, Investig. Radiol. 15 (1980) S61–S65 http://www.ncbi.nlm.nih.gov/pubmed/7203951.
[43] Y. Agmon, H. Peleg, Z. Greenfeld, S. Rosen, M. Brezis, Nitric oxide and prostanoids protect the renal outer medulla from radiocontrast toxicity in the rat, J. Clin. Invest. 94 (1994) 1069–1075, https://doi.org/10.1172/JCI117421.
[44] B.A. Molitoris, Urinary biomarkers: alone are they enough? Journal of the American Society of Nephrology: JASN 26 (2015) 1485–1488, https://doi.org/10.1681/ASN.2014111145.
[45] M. Fähling, E. Seeliger, A. Patzak, P.B. Persson, Understanding and preventing contrast-induced acute kidney injury, Nat. Rev. Nephrol. 13 (2017) 169–180, https://doi.org/10.1038/nrneph.2016.196.
[46] A. Leelahavanichkul, A.C.P. Souza, J.M. Street, V. Hsu, T. Tsuji, K. Doi, L. Li, X. Hu, H. Zhou, P. Kumar, J. Schnermann, R.A. Star, P.S.T. Yuen, Comparison of serum creatinine and serum cystatin C as biomarkers to detect sepsis-induced acute kidney injury and to predict mortality in CD-1 mice, American Journal of Physiology. Renal Physiology. 307 (2014) F939–F948, https://doi.org/10.1152/ajprenal.00025.2013.
[47] M. Andreucci, T. Faga, E. Riccio, M. Sabbatini, A. Pisani, A. Michael, The potential use of biomarkers in predicting contrast-induced acute kidney injury, Int. J. Nephrol. Renov. Dis. 9 (2016) 205–221, https://doi.org/10.2147/IJNRD.S105124.
[48] R.M. Subramaniam, C. Suarez-Cuervo, R.F. Wilson, S. Turban, A. Zhang, C. Sherrod, J. Aboagye, J. Eng, M.J. Choi, S. Hutfless, E.B. Bass, Effectiveness of prevention strategies for contrast-induced nephropathy: a systematic review and meta-analysis, Ann. Intern. Med. 164 (2016) 406–416, https://doi.org/10.7326/M15-1456.
[49] O. Toprak, M. Cirit, M. Tanrisev, C. Yazici, O. Canoz, M. Sipahioglu, A. Uzum, R. Ersoy, E.Y. Sozmen, Preventive effect of nebivolol on contrast-induced nephropathy in rats, Nephrology, Dialysis, Transplantation: Official Publication of the European Dialysis and Transplant Association - European Renal Association 23 (2008) 853–859, https://doi.org/10.1093/ndt/gfm691.
[50] E. Ari, A.E. Kedrah, Y. Alahdab, G. Bulut, Z. Eren, O. Baytekin, D. Odabasi, Antioxidant and renoprotective effects of paricalcitol on experimental contrast-induced nephropathy model, Br. J. Radiol. 85 (2012) 1038–1043, https://doi.org/10.1259/bjr/16327485.
[51] M.M. Tsamouri, M. Rapti, P. Kouka, C. Nepka, K. Tsarouhas, A. Soumelidis, G. Koukoulis, A. Tsatsakis, D. Kouretas, C. Tsitsimpikou, Histopathological evaluation and redox assessment in blood and kidney tissues in a rabbit contrast-induced nephrotoxicity model, Food Chem. Toxicol. 108 (2017) 186–193, https://doi.org/10.1016/j.fct.2017.07.058.
[52] K. Tsarouhas, C. Tsitsimpikou, X. Papantoni, D. Lazaridou, M. Koutouzis, S. Mazzaris, R. Rezaee, C. Mamoulakis, P. Georgoulias, C. Nepka, E. Rentoukas, Z. Kyriakides, A. Tsatsakis, D.A. Spandidos, D. Kouretas, Oxidative stress and kidney injury in trans-radial catheterization, Biomedical Reports 8 (2018) 417–425, https://doi.org/10.3892/br.2018.1071.
[53] W. Cao, F.F. Hou, J. Nie, AOPPs and the progression of kidney disease, Kidney International Supplements 4 (2014) 102–106, https://doi.org/10.1038/kisup.2014.19.
[54] L. Lin, G.-J. Zhao, L.-L. Qin, Association between advanced oxidation protein products (AOPP) and vascular calcification in uremic patients, Eur. Rev. Med. Pharmacol. Sci. 21 (2017) 4147–4152 http://www.ncbi.nlm.nih.gov/pubmed/29028083.
[55] V. Witko-Sarsat, V. Gausson, B. Descamps-Latscha, Are advanced oxidation protein products potential uremic toxins? Kidney Int. Suppl. (2003) S11–S14, https://doi.org/10.1046/j.1523-1755.63.s84.47.x.
[56] A.K. Koliada, D.S. Krasnenkov, A.M. Vaiserman, Telomeric aging: mitotic clock or stress indicator? Front. Genet. 6 (2015) 82, , https://doi.org/10.3389/fgene.2015.00082.
[57] M.A. Hamed, S.A. Ali, N.S. El-Rigal, Therapeutic potential of ginger against renal injury induced by carbon tetrachloride in rats., TheScientificWorldJournal 2012 (2012) 840421. doi:https://doi.org/10.1100/2012/840421.
[58] C. Soto, J. Pérez, V. García, E. Uría, M. Vadillo, L. Raya, Effect of silymarin on kidneys of rats suffering from alloxan-induced diabetes mellitus, Phytomedicine: International Journal of Phytotherapy and Phytopharmacology 17 (2010) 1090–1094, https://doi.org/10.1016/j.phymed.2010.04.011.
[59] R. Meng Bin Feng, Bin Huang, Y. Bi, S. Shen, D. Zhu, Silymarin protects against renal injury through normalization of lipid metabolism and mitochondrial biogenesis in high fat-fed mice, Free Radic. Biol. Med. 110 (2017) 240–249, https://doi.org/10.1016/j.freeradbiomed.2017.06.009.
[60] M. Colbay, S. Yuksel, I. Uslan, G. Acarturk, O. Karaman, O. Bas, H. Mollaoglu, M. Yagmurca, O.A. Ozen, Novel approach for the prevention of contrast nephropathy, Experimental and Toxicologic Pathology: Official Journal of the Gesellschaft Fur Toxikologische Pathologie 62 (2010) 81–89, https://doi.org/10.1016/j.etp.2009.02.119.
[61] C.-F. Chang, C.-C. Lin, Current concepts of contrast-induced nephropathy: a brief review, Journal of the Chinese Medical Association: JCMA 76 (2013) 673–681, https://doi.org/10.1016/j.jcma.2013.08.011.
[62] A. Levy, G. Cohen, E. Gilat, J. Kapon, S. Dachir, S. Abraham, M. Herskovitz, Z. Teitelbaum, L. Raveh, Extrapolating from animal studies to the efficacy in humans of a pretreatment combination against organophosphate poisoning, Arch. Toxicol. 81 (2007) 353–359, https://doi.org/10.1007/s00204-006-0153-6.
[63] C. Erdogan, O. Vang, Challenges in analyzing the biological effects of resveratrol, Nutrients. 8 (2016) 353, https://doi.org/10.3390/nu8060353.
[64] S. Reagan-Shaw, M. Nihal, N. Ahmad, Dose translation from animal to human studies revisited, FASEB Journal: Official Publication of the Federation of American Societies for Experimental Biology 22 (2008) 659–661, https://doi.org/10.1096/fj.07-9574LSF.
[65] A.B. Nair, S. Jacob, A simple practice guide for dose conversion between animals and human, Journal of Basic and Clinical Pharmacy 7 (2016) 27–31, https://doi.org/10.4103/0976-0105.177703.
[66] R.L. Hawke, S.J. Schrieber, T.A. Soule, Z. Wen, P.C. Smith, K.R. Reddy, A.S. Wahed, S.H. Belle, N.H. Afdhal, V.J. Navarro, J. Berman, Q.-Y. Liu, E. Doo, M.W. Fried, SyNCH Trial Group, Silymarin ascending multiple oral dosing phase I study in noncirrhotic patients with chronic hepatitis C, J. Clin. Pharmacol. 50 (2010) 434–449, https://doi.org/10.1177/0091270009347475.
[67] C. Tsitsimpikou, F. Vasilaki, K. Tsarouhas, P. Fragkiadaki, M. Tzardi, N. Goutzourelas, C. Nepka, A. Kalogeraki, I. Heretis, Z. Epitropaki, D. Kouretas, A.M. Tsatsakis, Nephrotoxicity in rabbits after long-term nandrolone decanoate administration, Toxicol. Lett. 259 (2016) 21–27, https://doi.org/10.1016/j.toxlet.2016.06.1122.
[68] C. Tsitsimpikou, M. Tzatzarakis, P. Fragkiadaki, L. Kovatsi, P. Stivaktakis, A. Kalogeraki, D. Kouretas, A.M. Tsatsakis, Histopathological lesions, oxidative stress and genotoxic effects in liver and kidneys following long term exposure of rabbits to diazinon and propoxur, Toxicology. 307 (2013) 109–114, https://doi.org/10.1016/j.tox.2012.11.002.